Response of Simulated Drinking Water Biofilm Mechanical and Structural Properties to Long-Term Disinfectant Exposure

Yun Shen,[†] Conghui Huang,[†] Guillermo L. Monroy,[‡] Dao Janjaroen,[†] Nicolas Derlon,[∥] Jie Lin,[†] Rosa Espinosa-Marzal,[†] Eberhard Morgenroth,[∥,⊥] Stephen A. Boppart,[‡,§] Nicholas J. Ashbolt,[#] Wen-Tso Liu,[†] and Thanh H. Nguyen*,[†]

[†]Department of Civil and Environmental Engineering, [‡]Department of Bioengineering, and [§]Department of Electrical and Computer Engineering, University of Illinois at Urbana–Champaign, Urbana, Illinois 61801, United States
[∥]Eawag: Swiss Federal Institute of Aquatic Science and Technology, 8600 Dübendorf, Switzerland
[⊥]Institute of Environmental Engineering, ETH Zürich, 8093 Zürich, Switzerland
[#]School of Public Health, University of Alberta, Edmonton, AB T6G 2G7 Canada

Ⓢ *Supporting Information*

ABSTRACT: Mechanical and structural properties of biofilms influence the accumulation and release of pathogens in drinking water distribution systems (DWDS). Thus, understanding how long-term residual disinfectants exposure affects biofilm mechanical and structural properties is a necessary aspect for pathogen risk assessment and control. In this study, elastic modulus and structure of groundwater biofilms was monitored by atomic force microscopy (AFM) and optical coherence tomography (OCT) during three months of exposure to monochloramine or free chlorine. After the first month of disinfectant exposure, the mean stiffness of monochloramine- or free-chlorine-treated biofilms was 4 to 9 times higher than those before treatment. Meanwhile, the biofilm thickness decreased from 120 ± 8 μm to $93 \pm 6-107 \pm$

Biofilms **RECOVERED** during long-term of disinfectant exposure

11 μm. The increased surface stiffness and decreased biofilm thickness within the first month of disinfectant exposure was presumably due to the consumption of biomass. However, by the second to third month during disinfectant exposure, the biofilm mean stiffness showed a 2- to 4-fold decrease, and the biofilm thickness increased to $110 \pm 7-129 \pm 8$ μm, suggesting that the biofilms adapted to disinfectant exposure. After three months of the disinfectant exposure process, the disinfected biofilms showed 2−5 times higher mean stiffness (as determined by AFM) and 6−13-fold higher ratios of protein over polysaccharide, as determined by differential staining and confocal laser scanning microscopy (CLSM), than the nondisinfected groundwater biofilms. However, the disinfected biofilms and nondisinfected biofilms showed statistically similar thicknesses (t test, $p > 0.05$), suggesting that long-term disinfection may not significantly remove net biomass. This study showed how biofilm mechanical and structural properties vary in response to a complex DWDS environment, which will contribute to further research on the risk assessment and control of biofilm-associated-pathogens in DWDS.
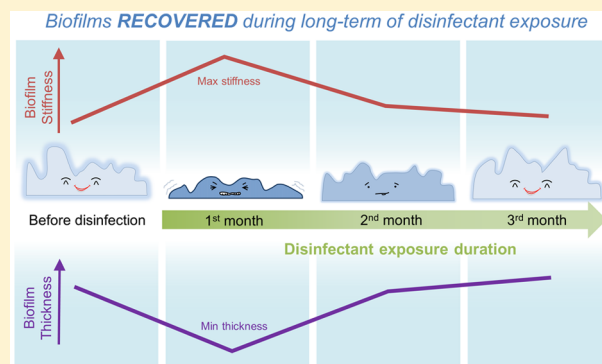
INTRODUCTION

Biofilms in drinking-water distribution systems (DWDS) can facilitate pathogen persistence and transmission[1] by harboring pathogens,[2] supplying nutrients,[3−7] and protecting pathogens from disinfection.[8,9] It is further reported that biofilms can capture or accumulate planktonic pathogens and then release these pathogens via the detached biofilm materials.[1] This process (biofilms accumulating and releasing pathogens) can be highly influenced by biofilm structural and mechanical properties. For example, biofilm roughness was observed to control pathogen accumulation to biofilms by increasing the interception of pathogens with biofilms.[10−13] Biofilm elasticity and cohesiveness are shown to be essential for the detachment of biofilms and biofilm-associated pathogens.[14−16] Therefore, comprehensive understanding of the mechanical and structural

properties for drinking water biofilms will provide information to predict, assess, and aid in controlling the risk of pathogens associated with DWDS biofilms.

A disinfectant residual is required in most drinking waters by the U.S. Environmental Protection Agency (EPA). Of particular interest here is that disinfectant residuals may influence the biofilm mechanical and structural properties through biomass loss and change in biofilm chemical composition. Thinner and rougher *Pseudomonas aeruginosa* biofilms were observed after a relatively short term (1−6 days) of continuous exposure to a

free-chlorine stream.[17] The cohesiveness of multispecies drinking water biofilms did not significantly change after 60 min of exposure to quiescent free-chlorine solution.[18] Longer disinfectant exposure (8 weeks) was also reported to lead to a reduction in groundwater biofilm thickness.[19] However, it is unknown how longer-term (i.e., normal operational) disinfectant exposure may influence mechanical and structural properties other than thickness. In addition to disinfectant exposure, hydrodynamic shear stress is known to influence biofilm mechanical and structural properties.[18,20−25] For example, biofilms developed under high shear stress up to 10 Pa were shown to be cohesively stronger.[15,21] The reduction of biofilm thickness was observed under a continuous exposure to shear stress up to 0.9 Pa.[21,22] During disinfectant exposure, shear can accelerate biofilm−disinfectant reaction by enhancing the mass transfer of disinfectant into the biofilms,[26] presumably leading to significant biofilm property variation. However, the combined effect of disinfectant exposure and shear stress on properties of biofilm grown under low-nutrient conditions over a longer time appears to be unreported.

To fill these research gaps, we monitored mechanical and structural properties of simulated drinking water biofilms during three months of disinfectant exposures. Monochloramine and free chlorine are the two most commonly used disinfectants in DWDS and were separately used to treat groundwater-grown biofilms. Both shear and quiescent conditions were explored during disinfectant exposure to simulate dynamic and stagnant zones in DWDS. In this study, we measured biofilm elastic modulus with atomic force microscopy (AFM) and biofilm structure (thickness and roughness) with optical coherence tomography (OCT) to determine the role of disinfectant exposure, shear conditions, and exposure duration time on biofilm mechanical and structural properties. The results of this study show how biofilm mechanical and structural properties vary in response to a complex DWDS environment and contribute to further research on the risk assessment and control of biofilm-associated-pathogens in DWDS.

■ MATERIALS AND METHODS

Biofilm Preparation and Disinfectant Exposure Assay. A groundwater source for drinking water in Urbana−Champaign, IL was selected for growing biofilms on PVC coupons (RD 128-PVC, BioSurface Technologies Corporation, Bozeman, MT) in CDC reactors (CBR 90−2, BioSurface Technologies Corporation), as described previously.[11,12] This groundwater source mainly contained 1.6 mM Ca^{2+}, 1.2 mM Mg^{2+}, and 1.0 mM Na^+. Continuous stirring at 125 rpm in the CDC reactors created a shear condition with a Reynolds (Re) number of 2384. The groundwater biofilms were developed in CDC reactors for one year and then distributed in six reactors for the subsequent biofilm disinfectant exposure.

In the biofilm disinfection step, these one-year-old biofilms were exposed to either free chlorine or monochloramine for 3 months. Specifically, groundwater containing 4 mg Cl_2/L of monochloramine or free chlorine were continuously introduced to the biofilm reactors in either stirred or nonstirred conditions (Figure 1). Reactors 1 and 4 were continuously exposed to groundwater containing freshly prepared monochloramine, and Reactors 2 and 5 were similarly exposed to freshly prepared free chlorine. Reactors 3 and 6 were exposed only to disinfectant-free groundwater and were used as controls. Reactors 1−3 were stirred at 125 rpm to simulate pipe flow conditions, and
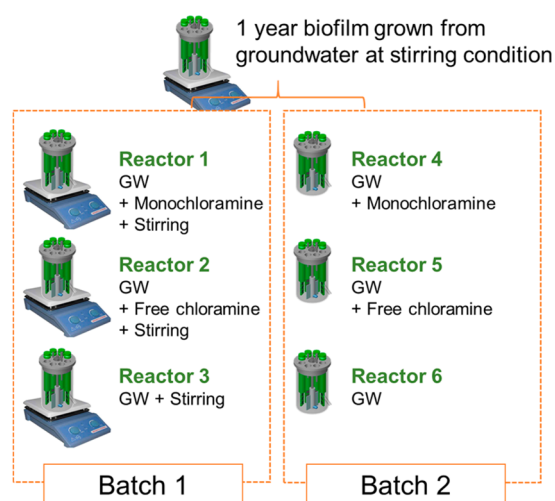

Figure 1. Experimental setup of disinfectant exposure assay for biofilms. GW: groundwater.

Reactors 4−6 were not stirred to simulate stagnant conditions. Both stirred and nonstirred conditions were used because the shear stress caused by stirring could influence the biofilm mechanical and structural properties.[18,20−25] In a real DWDS, both quiescent and shear conditions are likely to occur and affect biofilm structure. The six reactors were operated for 3 months at 4 mg Cl_2/L of total disinfectant, which is the maximal residual disinfectant concentration in DWDS required by the EPA. The feed disinfectant solutions were prepared and replenished every other day.

Biofilm Elastic Modulus Determination by AFM Indentation Test. *AFM Probe Preparation.* The indentation measurements were conducted with a silica sphere (with a diameter of 20 μm) glued to a tipless cantilever (calibrated with a normal spring constant of 0.6−1.2 N/m, Mikromasch, Lady's Island, SC). Similar to previous studies using spherical probes ranging in size from 10 to 50 μm to detect mechanical properties of polymers, cells, and biofilm,[27−29] spherical beads with a diameter of 20 μm (instead of a sharp tip (tip radius <10 nm)) were chosen to create larger contact areas and small contact pressures between the probe and the biofilm. A 20 μm diameter spherical probe can lead to a projected area of ∼54 μm^2 on a biofilm surface at the maximal indentation depth of 5 μm, determined on the basis of our measurements (e.g., a contact radius of ∼4.1 μm is obtained at a load of 52 nN for a rigid silica sphere and a flat biofilm of ∼5 kPa, according to the Hertz model).[30] Therefore, the 20 μm diameter spherical probe provided better representation of the biofilm elastic modulus at mesoscale compared with the submicron-scale measurement conducted by a AFM sharp tip. More details of building a spherical probe were described previously[31] and are also in the Supporting Information.

Indentation Test Data Collection and Analysis. The change in biofilm elastic modulus (Young's modulus) during the long-term disinfection process was estimated by indentation tests conducted on the same biofilm coupons from each reactor every month. The test biofilm coupons were carefully removed from the reactors for the indentation tests, after which they were immediately returned to the biofilm reactors. The biofilms were kept in groundwater during all the transit and experimental process to avoid dehydration. All of the indentation measurements were performed in groundwater
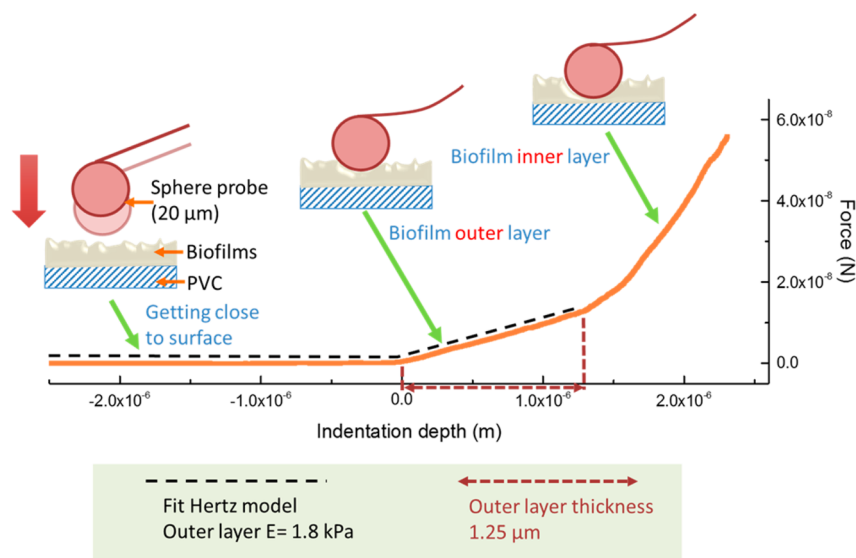
Figure 2. Indentation test principle. A sphere probe with the diameter of 20 μm was used in the indentation measurement. When the probe was indented into the biofilm surface, the deflection of the probe cantilever was monitored, and the applied force was calculated with the measured vertical deflection and the spring constant of the cantilever. The force as a function of indentation depth was then plotted, and the biofilm outer layer Young's modulus and thickness was determined accordingly.

filtered through a 0.22 μm cellulose membrane. The test biofilm coupons were gently rinsed with filtered groundwater three times before being subjected to indentation tests. The contact mode of an MFP-3D AFM (Asylum Research, Santa Barbara, CA) was used for all indentation tests. Before indentation, all AFM probes were calibrated on a bare glass surface both in air and in liquid to obtain the cantilever deflection sensitivity for force calculation.[27]

Following the probe calibration, the indentation tests were carried out with a probe approaching down velocity of 2 μm/s. The indentation force was measured as a function of indentation depth (Figure 2). The probe was indented into the biofilms with a maximal indentation depth of 5 μm. The indentation depths were limited within 10% of the total biofilm thickness to avoid the interference of the PVC substrate.[32,33] Prior to the probe contacting and indenting into the biofilms, surface forces, including electrical double layer, hydration, and steric interactions, between the probe and the biofilm can lead to a weak repulsion. The maximal range of the surface interaction was ~100 nm, determined on the basis of force measurements and its distinguishable force law; thus, a deconvolution of surface force and indentation force was possible in our measurements. After the probe overcame this weak surface repulsion, the probe penetrated (indented) into the biofilms at a certain depth dependent on the applied force (50−500 nN) and biofilm mechanical properties. In some indentation measurements, a bilayer biofilm structure was revealed along the indentation depth. The indentation curve for the biofilm outer layer has a lower slope compared to the biofilm inner layer (Figure 2), suggesting that the Young's modulus of the biofilm outer layer was reproducibly smaller than that of the biofilm inner layer. AFM indentation tests were also used to characterize the bilayer structure of other soft materials, such as cells.[27] The thickness of the outer layer was determined at the change of slope in the indentation curve (Figure 2), and the Young's modulus (E) of the shell layer was determined by fitting the curve to the Hertz model,[27] determined based on eq 1:

$$F = \frac{4}{3} \times \frac{E}{1 - v_s^2} \times \sqrt{r} \times \delta^{3/2}$$
(1)

where F is the force applied by the AFM probe to deform the biofilm surface, v_s is the biofilm Poisson's ratio (assumed to be 0.3[14]), r is the radius of the AFM probe, and δ is the probe indentation depth. The MFP-3D AFM software was used to conduct the indentation curve fitting using the Hertz model (fitting results have reduced chi-square values close to 1). The outer-layer Young's modulus was determined in this study because the outer layer directly exposed to drinking-water-phase is expected to be more relevant to pathogen accumulation and release processes, and the biofilm inner layer was not characterized here due to the possible interference of the PVC substrate.[32]

Indentation measurements were repeated at 20−30 randomly selected locations in each biofilm sample. At each location, indentation tests were conducted at different applied loads ranging from 50 to 500 nN. At each applied load, the indentation tests were repeated 2−5 times. In total, 120−450 indentation tests were conducted on each biofilm sample. Due to biofilm heterogeneity, the distribution of the Young's modulus values obtained from these randomly selected locations on each biofilm was analyzed to characterize the change in biofilm stiffness within a disinfectant exposure time period. Kolmogorov−Smirnov tests were used to compare the Young's modulus distributions obtained for different biofilms. In addition, all the measured values of Young's modulus for each sample were divided into four groups: a very soft group with $E < 5$ kPa, a soft group with 5 kPa$<E < 20$ kPa, a hard group with 20 kPa$<E < 100$ kPa, and a very hard group with 100 kPa $> E$. For each biofilm sample, the percentage of each group in all measured E values was determined.

Biofilm Structure Determination by Optical Coherence Tomography. The roughness and thickness of the biofilms were determined by the optical coherence tomography (OCT) technique described previously.[12,34] In this study, a custom-built 1300 nm based spectral domain OCT system imaged biofilm cross-sections of 3.1 mm transverse by 2.1 mm

in depth with an axial resolution of 4.2 μm and a transverse resolution of 3.9 μm.[35] To monitor the biofilm structural change, we collected the biofilms every week for the first month and every 2 weeks for the second and third month and subjected them to OCT imaging immediately after being removed from the reactor. A drop of groundwater was added on each biofilm coupon during OCT measurements to maintain the hydrated condition for biofilms. A volumetric scan consisting of two hundred images was taken in two separate locations from each sample. The average thickness and roughness were calculated from 20 randomly selected images for the biofilms in each reactor. ImageJ (http://imagej.nih.gov/ij/) was used to eliminate the background of these images before further analysis. Biofilm mean thickness and roughness were determined by analyzing gray scale gradient with automatic thresholding using the MATLAB program developed by Derlon et al.[36]

Biofilm Composition Determination by Confocal Laser Scanning Microscopy. To explore the possible connection between biofilm elasticity and biofilm composition, we determined the composition of three-months-disinfected biofilms and control biofilms by confocal laser scanning microscopy (CLSM; TCS SP2 RBB, Leica Microsystems). Biofilms are mainly composed of bacteria cells and extracellular polymeric substances (EPS). The biofilm mechanical properties are highly dependent on EPS. To determine the amount of each component in EPS, we used the fluorescent dyes of Sypro Orange and a mixture of ConA Alexa 633 and WGA Alexa 633 (Thermo Fisher Scientific Inc., Waltham, MA) to stain biofilm protein and polysaccharide, respectively. After this, the image of each component was scanned by CLSM, as described previously.[37] Briefly, the stained protein was scanned at the excitation wavelength of 470 nm and recorded at the emission wavelength of 570 nm. The stained polysaccharide was scanned at the excitation wavelength of 633 nm and recorded at the emission wavelength of 647 nm. A series of horizontal sections of protein and polysaccharide in the biofilms were imaged at an interval of 0.37 μm along the thickness of the biofilms. For each biofilm sample, 6−7 different locations with the size up to 720 × 720 μm were selected for CLSM imaging. To obtain the composition of the biofilms, we further analyzed the CLSM images of the biofilms using COMSTAT.[38,39] COMSTAT recognized the volume of protein and polysaccharide, respectively, by stacking each horizontal section image. The ratio of protein to polysaccharide was then determined accordingly. In this study, the volume of protein and polysaccharide determined by CLSM was not used to compare biofilm composition due to the heterogeneity in biofilm thickness and the possible diminishing of fluorescence signal along biofilm depth.[40] Instead, the ratios of protein over polysaccharide in biofilm EPS under different conditions were compared because these ratios reflected the change in biofilm EPS composition.

■ RESULTS

Biofilm Elastic Modulus Monitored by AFM at Different Disinfectant Exposure and Shear Conditions. To compare the biofilm mechanical properties after three months of exposure to different disinfectants and hydro-dynamics conditions, we obtained frequency distributions of the measured Young's moduli for the biofilms from different reactors. Compared to the E values of nondisinfected groundwater biofilms (reactors 3 and 6) (Figure 3a,b), the E
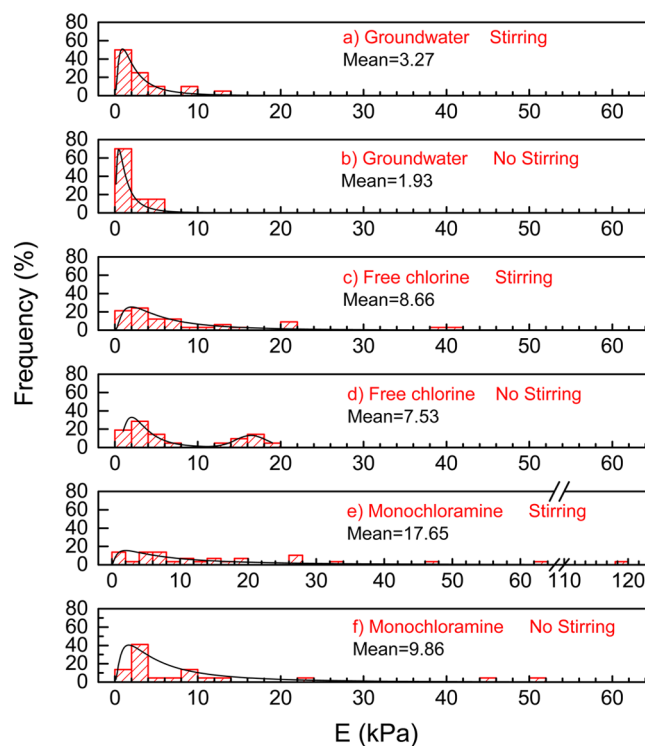

Figure 3. Frequency distribution of E for biofilm after 3 months exposure of groundwater (a) with and (b) without stirring, free chlorine (c) with and (d) without stirring, and monochloramine (e) with and (f) without stirring, respectively. The Y-axis represents the frequency of occurrences of E values with each interval size of 5 kPa.

values of free-chlorine- (Figure 3c,d) and monochloramine-treated biofilms (Figure 3e,f) clustered in a higher range (Kolmogorov−Smirnov test, $p < 0.05$). For example, under the nonstirring (shear-free) condition (Figure 3b,d,f), the maximal E frequency for the groundwater biofilms was located in the lower range of 0−2 kPa, and for the free-chlorine- or monochloramine-treated biofilms, the maximal E frequency was located in the higher range of 2−4 kPa. E distributing in the higher ranges indicated that exposure to free chlorine and monochloramine increased the biofilm Young's modulus or stiffness. In addition, the E distributions under the stirring (shear) and nonstirring (shear-free) conditions were compared. For the groundwater biofilms and free-chlorine-treated biofilms (Figure 3a versus Figure 3b and Figure 3c versus Figure 3d), the E distributions under the stirring and nonstirring conditions were statistically the same (Kolmogorov−Smirnov test: $p > 0.05$), indicating that moderate hydrodynamic shear did not significantly alter the biofilm Young's modulus after three months of disinfectant-free groundwater or free chlorine exposure. Conversely, the monochloramine-treated biofilms indicated that a shear condition during monochloramine exposure increased the biofilm elastic modulus (Figure 3e versus Figure 3f), given the statistically different E distributions (Kolmogorov−Smirnov test, $p = 0.04$). In summary, both free-chlorine and monochloramine treatment increased the Young's modulus E or stiffness of the biofilms, and the shear condition increased biofilm stiffness only under the monochloramine exposure condition.

In addition to examining the biofilm Young's modulus under different disinfectant exposure and shear conditions, the change in the Young's modulus over disinfectant exposure time was

also determined (Figure 4). Before disinfection treatment, all of the measured Young's modulus values belonged to either the
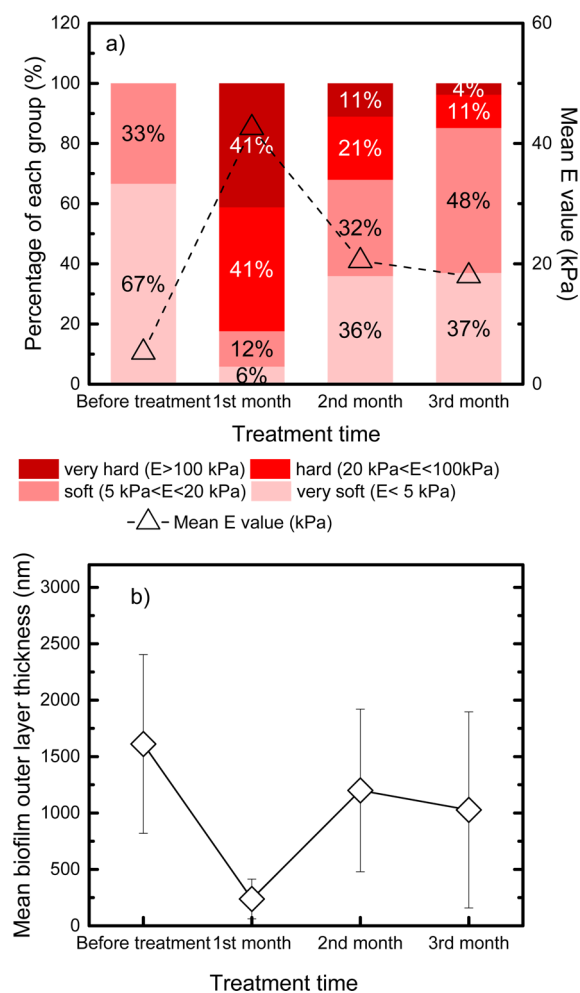

Figure 4. (a) The percentage stacked bar for the Young modulus and (b) the outer layer thickness of biofilms during the three months of monochloramine treatment under stirring conditions. The red line in panel a shows the mean value of E at each time point. The percentage stacked bars and outer layer thicknesses of biofilms during other treatment conditions are shown in Figure S1 (free-chlorine treatment under stirring conditions), Figure S2 (monochloramine treatment under nonstirring conditions), and Figure S3 (free-chlorine treatment under nonstirring conditions).

very soft or the soft group (E values smaller than 20 kPa). However, after one month of monochloramine treatment, the fraction of soft and very soft biofilms in the measured biofilms was reduced to 18%. Most of these biofilms were hard (20 kPa $< E <$ 100 kPa) or very hard ($E >$ 100 kPa). The mean value of E after one month of monochloramine disinfection was eight times higher than that before treatment (42 kPa versus 5 kPa). The increased E values suggested that the biofilm stiffness was significantly increased after monochloramine exposure. However, after two or three months of exposure to monochloramine, soft and very soft biofilms again dominated the overall biofilm behavior. The fraction of soft and very soft biofilms in the total measured biofilms increased to 68% and 85% at the second and third month, respectively. The E values at the second and third month were statistically similar (t test, $p =$ 0.73) and the mean E values were twice lower than that for the

first month, suggesting that the biofilm stiffness decreased in the second month and then stabilized by the third month. The observation that E increased in the first month of disinfectant treatment and then decreased in the following months was also observed for other disinfection treatment conditions (Figure S1a, Figure S2a, and Figure S3a). Thus, the biofilm stiffness increased after one month of disinfectant exposure, but it decreased and became stable with longer disinfection treatment (2 or 3 months).

The above trend for the Young's modulus change over time was the reverse of the trend in average biofilm outer layer thickness (Figure 4, Figure S1, Figure S2, and Figure S3). As shown in Figure 4, the highest biofilm Young's modulus (Figure 4a) and the lowest biofilm outer-layer thickness (Figure 4b) was observed at the first month during exposure to monochloramine with shear conditions. Similar observation of the highest E value corresponding to the lowest average biofilm outer layer thickness was also found for the biofilms under other disinfectant exposure and shear conditions (Figure S1, Figure S2, and Figure S3).

Biofilm Structure Monitored by OCT at Different Disinfectant Exposure and Shear Conditions. The average thickness of biofilms after three months of exposure to different disinfectant and shear conditions was estimated using OCT (Figure S4a). There was no significant difference between biofilms with or without disinfectant exposure. Specifically, under shear conditions, all the monochloramine-treated, free-chlorine-treated, and nondisinfected (control) groundwater biofilms had statistically similar thicknesses (129 ± 8, 127 ± 19, and 123 ± 18 μm, respectively; t test, $p >$ 0.05). However, under shear-free conditions, although the free-chlorine-treated and groundwater biofilms still had statistically similar thicknesses (117 ± 6 μm versus 118 ± 10 μm; t test, p = 0.75), the monochloramine-treated biofilms had a slightly lower biofilm thickness of 110 ± 7 μm (t test, both $p <$ 0.05). The similarity of thicknesses for the disinfected and nondisinfected biofilms suggested that three months of disinfection did not significantly reduce biofilm thickness. In addition, no apparent biofilm thickness change was measured under different hydrodynamic conditions for free-chlorine-treated biofilms and nondisinfected biofilms (t test, both $p >$ 0.05). Nonetheless, the thicknesses of monochloramine-treated biofilms under the shear condition were higher than those under the shear-free condition (t test, p = 2.5×10^{-8}). Overall, however, monochloramine- and free-chlorine-treated biofilms did not show substantially lower thickness than the nontreated biofilms.

In addition to comparing the biofilm thickness under different disinfectant exposure and shear conditions, we also monitored the change in biofilm average thickness over the three months of disinfectant exposure (Table S1). A decrease in thickness under monochloramine treatment over the first 5 weeks of disinfection was observed (t test, $p <$ 0.05), followed by an increase in thickness over the next 8 weeks (t test, $p <$ 0.05). The lowest biofilm thicknesses were observed at the fifth week for the monochloramine-treated biofilm under the shear (105 ± 6 μm) and the shear-free conditions (93 ± 6 μm). For the free-chlorine-treated biofilm, the thinnest biofilm thickness was observed at the fourth week, with thickness values of 107 ± 11 μm and 103 ± 8 μm under shear and shear-free conditions, respectively. In the following weeks (5th to 13th week), the thickness increased and then recovered to the initial thickness at the end of disinfectant exposure (biofilm thickness at week 0 versus biofilm thickness at week 13; t test; $p >$ 0.05). Although

the monochloramine and free-chlorine exposure showed the lowest thickness at around month 1 (4th or 5th week), the nondisinfected groundwater biofilms did not show significant change in thickness over the 3 month study, under either shear or shear-free conditions (t test, $p > 0.05$). Therefore, biofilm thickness decreased during a short-term of disinfectant exposure (roughly one month), but the thickness increased over the rest of the disinfectant exposure period.

The biofilm roughness from each reactor was compared after three months of disinfectant exposure (Figure S4b). Under the same hydrodynamic conditions (shear or shear-free), the monochloramine-treated biofilms showed statistically lower roughness than free-chlorine-treated biofilms (t test, $p < 0.05$). In addition, with the same disinfectant treatment, the biofilm roughness under the shear condition was significantly lower than that under the shear-free condition. For example, the roughness for the monochloramine-treated biofilms was 0.15 ± 0.03 and 0.36 ± 0.04 under the shear and the shear-free conditions (t test, p = 1.6×10^{-20}), respectively (Figure 5). Therefore, for the biofilms exposed to the same disinfectant, the shear condition led to significantly lower biofilm roughness than the shear-free condition.
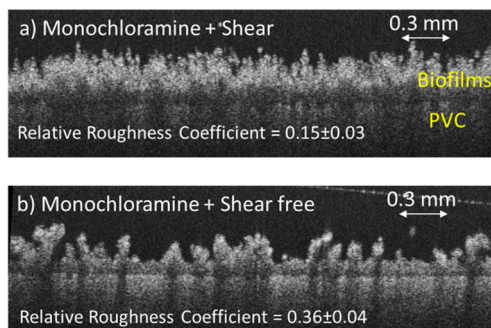

Figure 5. OCT images of monochloramine-treated, free-chlorine-treated, and groundwater biofilms under shear conditions.

The change of biofilm roughness over the three months of disinfectant exposure was also monitored (Table S2). Under the shear condition, roughness of monochloramine-treated biofilms showed a 1.7-fold decrease in the first 4 weeks and then remained constant in the following 9 weeks. The roughness of nondisinfected groundwater biofilms also decreased 1.3-fold over the three months under the same shear condition. However, the free-chlorine-treated biofilms kept the statistically similar roughness before and after the three months of disinfection (0.25 ± 0.02 versus 0.26 ± 0.05; t test, p = 0.25). Under the shear-free condition, roughness of all monochloramine-treated, free-chlorine-treated, and nondisinfected biofilms kept increasing during the three-month experiment. For example, the biofilm roughness increased 1.4 times during monochloramine exposure. In summary, under shear conditions, the biofilm roughness was reduced or did not change by the three-month experiment. In contrast, with stagnant conditions, the roughness increased for all examined treatment conditions.

Biofilm Composition after Long-Term Disinfection Determined by CLSM. The ratio of protein over polysaccharide in biofilm EPS under different conditions was determined by CLSM after the three months of disinfectant exposure. For the biofilms without any disinfectant exposure, the ratios of protein/polysaccharide were 1.2 ± 0.46 and $0.92 \pm$

0.34 under shear and shear-free conditions, respectively. However, with the free chlorine exposure, the biofilms had protein to polysaccharide ratios of 6.29 ± 3.19 and 6.66 ± 3.58, significantly higher than those of groundwater biofilms (t test, $p < 0.05$). With monochloramine exposure, these protein to polysaccharide ratios were further increased (t test, $p < 0.05$), being 13.09 ± 1.89 and 8.28 ± 2.47, respectively. These higher protein to polysaccharide ratios after disinfectant exposure suggested that free chlorine and monochloramine either directly consumed more polysaccharide than protein in biofilm EPS or stimulated changes in the biofilm community that were expressed the different ratios.

■ DISCUSSION

In contrast to previous studies focusing on short-term exposure of biofilms to disinfectants,[17,18] our three-month disinfectant exposure study revealed the dynamics of biofilm structural and mechanical properties. Specifically, the least biofilm thickness and the highest stiffness were observed after one month of disinfectant exposure, but these properties recovered after three months. To our best knowledge, this is the first report revealing how biofilm properties changed during a long-term disinfection. In the first month of disinfectant exposure, a decrease of $13-27$ μm in overall biofilm thickness was observed, suggesting biomass consumption by disinfectant. In addition, an increase from 4 to 9 times in the biofilm stiffness together with reduction in the biofilm outer layer thickness in the first month may be attributed to the consumption of biofilm EPS by disinfectant in the outer layer and the lack of EPS production by the inactivated bacteria cells near the outer layer. However, with longer disinfectant exposure, the biofilms may adapt themselves to the disinfectant (e.g., by adjusting their microbial community[19,41]) and produce EPS again to replenish the outer layer, consistent with the observed increase ($14-35$ μm) of the biofilm thickness and decrease (2-fold to 4-fold) of the biofilm stiffness. Thus, although short-term disinfection can lead to thinner and stiffer biofilms, biofilms could recover with long-term disinfectant exposure, a condition relevant for DWDS.

The long-term disinfectant exposure did not lead to a significant difference of biofilm thickness between the disinfected and nondisinfected biofilms, but higher stiffness was observed for disinfected biofilms compared with non-disinfected biofilms. The thickness between disinfected and nondisinfected biofilms was similar, presumably because the biofilms became resistant to disinfectant under a long-term disinfection. Specifically, certain microorganisms in biofilms could become more resistant to disinfection.[42] Also, disinfectant exposure could generate selective pressure to certain microbial populations in biofilms.[43,44] Hence, after three months of disinfection, neither monochloramine- nor free-chlorine-treated biofilms showed obvious differences from the nondisinfected groundwater biofilms. Unlike biofilm thickness, the biofilm stiffness of the disinfected biofilms were $3-5$ times higher than that of the nondisinfected biofilms. This higher biofilm stiffness was observed together with higher ratios of protein over polysaccharide, suggesting that the higher stiffness of the biofilms after disinfection exposure may be due to the higher fraction of EPS protein. A previous study also suggested that protein-rich regions on the *Lactobacillus johnsonii* bacteria surface were stiffer than that of polysaccharide-rich regions.[45] Because stiffer biofilms may be more stable against shear stress,[16] less detachment and release of biofilm-associated pathogens in DWDS would be expected. Therefore, although

long-term disinfection could not significantly remove biofilms, less detachment of stiffened biofilms is expected.

Shear conditions during disinfectant exposure can also influence biofilm structural and mechanical properties. Compared to biofilms treated under shear-free conditions, the biofilms exposed to shear conditions were smoother due to the biofilm erosion caused by shear stress.[14] These smoother biofilms were expected to be more resistant to shear force and detachment.[46] In addition, shear stress during monochloramine exposure caused stiffer biofilms. A previous numerical modeling study of the biofilm mechanical behavior showed that shear stress compressed and reduced the voids inside biofilms, thus leading to more compact and stiffer biofilms.[47] However, no internal voids or channels were observed in this study under the resolution of the OCT imaging system used. Other studies revealed the enhanced disinfectant mass transfer by shear,[48,49] which may also cause the enhanced disinfection reaction and thus an increase in biofilm stiffness under shear stress. However, the stiffness of free-chlorine-treated biofilms under shear and shear-free conditions did not show any difference, suggesting that other factors, such as limited penetration of chlorine,[50] may control the mechanical properties of these biofilms.

In this study, the evolution of the biofilm Young's modulus during three months of exposure to disinfectants was characterized by AFM microindentation. A wide range of values for the Young's modulus has been reported in previous studies due to the use of diverse methods and biofilms.[51−60] Most of the studies that used AFM nano- or microindentation to determine the Young's modulus focused on single-culture biofilms and revealed a biofilm Young's modulus ranging from 0.1 to 316 kPa.[51,58,59,61] Only one study applied nanoindentation to drinking water biofilms and reported a biofilm Young's modulus greater than 200 kPa.[51] In our study, the lowest biofilm Young's modulus was found to be 0.3 kPa (for nondisinfected biofilms), and the highest biofilm Young's modulus was 179 kPa (for monochloramine-treated biofilms). These values are within the range of previously reported biofilm Young's modulus.

Our study applied AFM microindentation on multiculture biofilms, providing a promising and nondestructive way to determine microscale drinking-water biofilm mechanical properties in a liquid environment. However, AFM indentation has some limitations in determining the mechanical behavior of biofilms, including that (1) only the elastic modulus of the outer layer can be quantitatively determined. Although a stiffer biofilm inner layer was revealed in the indentation curves and previous studies,[47,62] it was not characterized by indentation owing to relevant substrate effects; (2) the elastic modulus could only be measured along the biofilm depth but not in the lateral direction. However, a certain anisotropy of the biofilm is expected; (3) the shear modulus is also essential to determine biofilm resistance under shear stress, and it cannot be determined from AFM microindentation. To overcome these limitations, we could combined other techniques with AFM indentation. For example, rheometers and tensile tests could be used to measure the mesoscale biofilm main-body mechanical properties,[53,56,60,63−65] and AFM sharp tips could be used to abrade biofilm and explore biofilm mechanical strength along the horizontal direction.[15,18] Future efforts will focus on taking advantage of multiple techniques to comprehensively characterize the bulk mechanical behavior of biofilms.

■ IMPLICATIONS

The results of this study on biofilm mechanical and structural properties under long-term disinfectant exposure provide insights on pathogen transmission prediction and control in DWDS. Specifically, the biofilm elastic modulus and structure measurement results suggested that (1) more rigid biofilms after long-term disinfectant exposure may be more resistant to detachment, which can thus reduce the release of biofilm-associated pathogens; (2) shear stress in DWDS could help to maintain relatively smoother biofilms, on which less pathogen accumulation and biofilm detachment is expected; (3) disinfectant exposure in one month would have the best effect on increasing biofilm stiffness and reducing biofilm thickness, and longer time disinfection will lead to a decrease of biofilm stiffness and a recovery of biofilm thickness. Accordingly, risk assessment on DWDS pathogens could incorporate the information on biofilm mechanical and structural properties to precisely evaluate the biofilm-associated pathogen release level under disinfectant-exposure conditions. In the next step, the connection between pathogen transmission and long-term disinfected biofilms needs to be further explored, and a mathematical model will be built to estimate the risk of pathogens in DWDS with disinfectant exposure.

■ ASSOCIATED CONTENT

ⓢ Supporting Information

The Supporting Information is available free of charge on the ACS Publications website at DOI: 10.1021/acs.est.5b04653.

> Additional details regarding sphere probe preparation, examination of AFM probe contamination, and statistical analysis. Figures showing the percentage stacked bar and the outer layer thickness of biofilms during the 3 months of free chlorine and monochloramine treatment under stirring and no-stirring conditions; average thickness and relative roughness coefficient of biofilms after 3 months of exposure to monochloramine, free chlorine, and groundwater without disinfectant under shearing and no-shearing conditions, respectively; and calibration force−distance curves obtained in water on clean glass surfaces. Tables showing the change of biofilm average thickness and relative roughness during the disinfectant exposure under different treatments. (PDF)

■ AUTHOR INFORMATION

Notes

The authors declare no competing financial interest.

■ ACKNOWLEDGMENTS

■ REFERENCES

(1) Lau, H.; Ashbolt, N. The role of biofilms and protozoa in *Legionella pathogenesis*: implications for drinking water. *J. Appl. Microbiol.* **2009**, *107* (2), 368−378.

(2) Ashbolt, N. J. Environmental (saprozoic) pathogens of engineered water systems: understanding their ecology for risk assessment and management. *Pathogens* **2015**, *4* (2), 390−405.

(3) Tison, D.; Pope, D.; Cherry, W.; Fliermans, C. Growth of *Legionella pneumophila* in association with blue-green algae (cyanobacteria). *Appl. Environ. Microbiol.* **1980**, *39* (2), 456−459.

(4) Wadowsky, R. M.; Yee, R. B. Satellite growth of *Legionella-pneumophila* with an environmental isolate of *Flavobacterium-breve*. *Appl. Environ. Microbiol.* **1983**, *46* (6), 1447−1449.

(5) Stout, J. E.; Yu, V. L.; Best, M. G. Ecology of *Legionella pneumophila* within water distribution systems. *Appl. Environ. Microbiol.* **1985**, *49* (1), 221−228.

(6) Temmerman, R.; Vervaeren, H.; Noseda, B.; Boon, N.; Verstraete, W. Necrotrophic growth of *Legionella pneumophila*. *Appl. Environ. Microbiol.* **2006**, *72* (6), 4323−4328.

(7) Thomas, J. M.; Ashbolt, N. J. Do free-living amoebae in treated drinking water systems present an emerging health risk? *Environ. Sci. Technol.* **2011**, *45* (3), 860−869.

(8) Cargill, K. L.; Pyle, B. H.; Sauer, R. L.; McFeters, G. A. Effects of culture conditions and biofilm formation on the iodine susceptibility of *Legionella pneumophila*. *Can. J. Microbiol.* **1992**, *38* (5), 423−429.

(9) Cooper, I. R.; Hanlon, G. W. Resistance of *Legionella pneumophila* serotype 1 biofilms to chlorine-based disinfection. *J. Hosp. Infect.* **2010**, *74* (2), 152−159.

(10) Hassan, M. F.; Lee, H. P.; Lim, S. P. Effects of shear and surface roughness on reducing the attachment of *Oscillatoria sp* filaments on substrates. *Water Environ. Res.* **2012**, *84* (9), 744−752.

(11) Janjaroen, D.; Ling, F.; Monroy, G.; Derlon, N.; Mogenroth, E.; Boppart, S. A.; Liu, W. T.; Nguyen, T. H. Roles of ionic strength and biofilm roughness on adhesion kinetics of *Escherichia coli* onto groundwater biofilm grown on PVC surfaces. *Water Res.* **2013**, *47* (7), 2531−42.

(12) Shen, Y.; Monroy, G. L.; Derlon, N.; Janjaroen, D.; Huang, C.; Morgenroth, E.; Boppart, S. A.; Ashbolt, N. J.; Liu, W.-T.; Nguyen, T. H. Role of biofilm roughness and hydrodynamic conditions in *Legionella pneumophila* adhesion to and detachment from simulated drinking water biofilms. *Environ. Sci. Technol.* **2015**, *49* (7), 4274−4282.

(13) Wu, M.-Y.; Sendamangalam, V.; Xue, Z.; Seo, Y. The influence of biofilm structure and total interaction energy on *Escherichia coli* retention by *Pseudomonas aeruginosa* biofilm. *Biofouling* **2012**, *28* (10), 1119−1128.

(14) Picioreanu, C.; van Loosdrecht, M. C.; Heijnen, J. J. Two-dimensional model of biofilm detachment caused by internal stress from liquid flow. *Biotechnol. Bioeng.* **2001**, *72* (2), 205−218.

(15) Ahimou, F.; Semmens, M. J.; Novak, P. J.; Haugstad, G. Biofilm cohesiveness measurement using a novel atomic force microscopy methodology. *Appl. Environ. Microbiol.* **2007**, *73* (9), 2897−2904.

(16) Tierra, G.; Pavissich, J. P.; Nerenberg, R.; Xu, Z.; Alber, M. S. Multicomponent model of deformation and detachment of a biofilm under fluid flow. *J. R. Soc., Interface* **2015**, *12* (106), 20150045.

(17) Xue, Z.; Seo, Y. Impact of chlorine disinfection on redistribution of cell clusters from biofilms. *Environ. Sci. Technol.* **2013**, *47* (3), 1365−1372.

(18) Mathieu, L.; Bertrand, I.; Abe, Y.; Angel, E.; Block, J. C.; Skali-Lami, S.; Francius, G. Drinking water biofilm cohesiveness changes under chlorination or hydrodynamic stress. *Water Res.* **2014**, *55* (0), 175−184.

(19) Ling, F.; Liu, W.-T. Impact of chloramination on the development of laboratory-grown biofilms fed with filter-pretreated groundwater. *Microbes Environ.* **2013**, *28* (1), 50−57.

(20) Stoodley, P.; Cargo, R.; Rupp, C.; Wilson, S.; Klapper, I. Biofilm material properties as related to shear-induced deformation and detachment phenomena. *J. Ind. Microbiol. Biotechnol.* **2002**, *29* (6), 361−367.

(21) Huang, Z.; McLamore, E.; Chuang, H.; Zhang, W.; Wereley, S.; Leon, J.; Banks, M. Shear-induced detachment of biofilms from hollow fiber silicone membranes. *Biotechnol. Bioeng.* **2013**, *110* (2), 525−534.

(22) Chang, H. T.; Rittmann, B. E.; Amar, D.; Heim, R.; Ehlinger, O.; Lesty, Y. Biofilm detachment mechanisms in a liquid-fluidized bed. *Biotechnol. Bioeng.* **1991**, *38* (5), 499−506.

(23) Vieira, M. J.; Melo, L. F.; Pinheiro, M. M. Biofilm formation: hydrodynamic effects on internal diffusion and structure. *Biofouling* **1993**, *7* (1), 67−80.

(24) Peyton, B. M. Effects of shear stress and substrate loading rate on *Pseudomonas aeruginosa* biofilm thickness and density. *Water Res.* **1996**, *30* (1), 29−36.

(25) Liu, Y.; Tay, J.-H. The essential role of hydrodynamic shear force in the formation of biofilm and granular sludge. *Water Res.* **2002**, *36* (7), 1653−1665.

(26) Clark, M. M. *Transport modeling for environmental engineers and scientists*. John Wiley & Sons: Hoboken, NJ, 2012.

(27) Carl, P.; Schillers, H. Elasticity measurement of living cells with an atomic force microscope: data acquisition and processing. *Pfluegers Arch.* **2008**, *457* (2), 551−559.

(28) Wiesinger, A.; Peters, W.; Chappell, D.; Kentrup, D.; Reuter, S.; Pavenstädt, H.; Oberleithner, H.; Kümpers, P. Nanomechanics of the endothelial glycocalyx in experimental sepsis. *PLoS One* **2013**, *8* (11), e80905.

(29) Lau, P. C. Y.; Dutcher, J. R.; Beveridge, T. J.; Lam, J. S. Absolute quantitation of bacterial biofilm adhesion and viscoelasticity by microbead force spectroscopy. *Biophys. J.* **2009**, *96* (7), 2935−2948.

(30) Johnson, K.; Kendall, K.; Roberts, A. In Surface Energy and the Contact of Elastic Solids, *Proc. R. Soc. London, Ser. A*, 1971; pp 301−313.

(31) Li, A.; Ramakrishna, S. N.; Kooij, E. S.; Espinosa-Marzal, R. M.; Spencer, N. D. Poly(acrylamide) films at the solvent-induced glass transition: adhesion, tribology, and the influence of crosslinking. *Soft Matter* **2012**, *8* (35), 9092−9100.

(32) Oliver, W. C.; Pharr, G. M. An improved technique for determining hardness and elastic modulus using load and displacement sensing indentation experiments. *J. Mater. Res.* **1992**, *7* (06), 1564−1583.

(33) Saha, R.; Nix, W. D. Effects of the substrate on the determination of thin film mechanical properties by nanoindentation. *Acta Mater.* **2002**, *50* (1), 23−38.

(34) Xi, C.; Marks, D.; Schlachter, S.; Luo, W.; Boppart, S. A. High-resolution three-dimensional imaging of biofilm development using optical coherence tomography. *J. Biomed. Opt.* **2006**, *11* (3), 34001.

(35) Ahmad, A.; Shemonski, N. D.; Adie, S. G.; Kim, H.-S.; Hwu, W.-M. W.; Carney, P. S.; Boppart, S. A. Real-time in vivo computed optical interferometric tomography. *Nat. Photonics* **2013**, *7* (6), 444−448.

(36) Derlon, N.; Peter-Varbanets, M.; Scheidegger, A.; Pronk, W.; Morgenroth, E. Predation influences the structure of biofilm developed on ultrafiltration membranes. *Water Res.* **2012**, *46* (10), 3323−3333.

(37) Xue, Z.; Lee, W. H.; Coburn, K. M.; Seo, Y. Selective reactivity of monochloramine with extracellular matrix components affects the disinfection of biofilm and detached clusters. *Environ. Sci. Technol.* **2014**, *48* (7), 3832−3839.

(38) Heydorn, A.; Ersbøll, B. K.; Hentzer, M.; Parsek, M. R.; Givskov, M.; Molin, S. Experimental reproducibility in flow-chamber biofilms. *Microbiology* **2000**, *146* (10), 2409−2415.

(39) Heydorn, A.; Nielsen, A. T.; Hentzer, M.; Sternberg, C.; Givskov, M.; Ersbøll, B. K.; Molin, S. Quantification of biofilm structures by the novel computer program comstat. *Microbiology* **2000**, *146* (10), 2395−2407.

(40) Vroom, J. M.; De Grauw, K. J.; Gerritsen, H. C.; Bradshaw, D. J.; Marsh, P. D.; Watson, G. K.; Birmingham, J. J.; Allison, C. Depth penetration and detection of pH gradients in biofilms by two-photon excitation microscopy. *Appl. Environ. Microbiol.* **1999**, *65* (8), 3502−3511.

(41) Revetta, R. P.; Gomez-Alvarez, V.; Gerke, T. L.; Curioso, C.; Santo Domingo, J. W.; Ashbolt, N. J. Establishment and early succession of bacterial communities in monochloramine-treated drinking water biofilms. *FEMS Microbiol. Ecol.* **2013**, *86* (3), 404−414.

(42) Miller, H. C.; Wylie, J.; Dejean, G.; Kaksonen, A. H.; Sutton, D.; Braun, K.; Puzon, G. J. Reduced efficiency of chlorine disinfection of *Naegleria Fowleri* in a drinking water distribution biofilm. *Environ. Sci. Technol.* **2015**, *49* (18), 11125−11131.

(43) Gomez-Alvarez, V.; Schrantz, K. A.; Pressman, J. G.; Wahman, D. G. Biofilm community dynamics in bench-scale annular reactors simulating arrestment of chloraminated drinking water nitrification. *Environ. Sci. Technol.* **2014**, *48* (10), 5448−5457.

(44) Roeder, R. S.; Lenz, J.; Tarne, P.; Gebel, J.; Exner, M.; Szewzyk, U. Long-term effects of disinfectants on the community composition of drinking water biofilms. *Int. J. Hyg. Environ. Health* **2010**, *213* (3), 183−189.

(45) Schaer-Zammaretti, P.; Ubbink, J. Imaging of lactic acid bacteria with AFM—elasticity and adhesion maps and their relationship to biological and structural data. *Ultramicroscopy* **2003**, *97* (1), 199−208.

(46) Van Loosdrecht, M.; Eikelboom, D.; Gjaltema, A.; Mulder, A.; Tijhuis, L.; Heijnen, J. Biofilm structures. *Water Sci. Technol.* **1995**, *32* (8), 35−43.

(47) Laspidou, C.; Spyrou, L.; Aravas, N.; Rittmann, B. Material modeling of biofilm mechanical properties. *Math. Biosci.* **2014**, *251*, 11−15.

(48) Bishop, P. L.; Gibbs, J. T.; Cunningham, B. E. Relationship between concentration and hydrodynamic boundary layers over biofilms. *Environ. Technol.* **1997**, *18* (4), 375−385.

(49) Wäsche, S.; Horn, H.; Hempel, D. C. Influence of growth conditions on biofilm development and mass transfer at the bulk/biofilm interface. *Water Res.* **2002**, *36* (19), 4775−4784.

(50) Lee, W. H.; Wahman, D. G.; Bishop, P. L.; Pressman, J. G. Free chlorine and monochloramine application to nitrifying biofilm: comparison of biofilm penetration, activity, and viability. *Environ. Sci. Technol.* **2011**, *45* (4), 1412−1419.

(51) Abe, Y.; Polyakov, P.; Skali-Lami, S.; Francius, G. Elasticity and physico-chemical properties during drinking water biofilm formation. *Biofouling* **2011**, *27* (7), 739−750.

(52) Aggarwal, S.; Hozalski, R. M. Determination of biofilm mechanical properties from tensile tests performed using a micro-cantilever method. *Biofouling* **2010**, *26* (4), 479−486.

(53) Aggarwal, S.; Poppele, E. H.; Hozalski, R. M. Development and testing of a novel microcantilever technique for measuring the cohesive strength of intact biofilms. *Biotechnol. Bioeng.* **2010**, *105* (5), 924−934.

(54) Blauert, F.; Horn, H.; Wagner, M. Time-resolved biofilm deformation measurements using optical coherence tomography. *Biotechnol. Bioeng.* **2015**, *112* (9), 1893−1905.

(55) Cense, A. W.; Peeters, E. A. G.; Gottenbos, B.; Baaijens, F. P. T.; Nuijs, A. M.; Van Dongen, M. E. H. Mechanical properties and failure of *Streptococcus* mutans biofilms, studied using a microindentation device. *J. Microbiol. Methods* **2006**, *67* (3), 463−472.

(56) Hohne, D. N.; Younger, J. G.; Solomon, M. J. Flexible microfluidic device for mechanical property characterization of soft viscoelastic solids such as bacterial biofilms. *Langmuir* **2009**, *25* (13), 7743−7751.

(57) Mathias, J. D.; Stoodley, P. Applying the digital image correlation method to estimate the mechanical properties of bacterial biofilms subjected to a wall shear stress. *Biofouling* **2009**, *25* (8), 695−703.

(58) Mosier, A. P.; Kaloyeros, A. E.; Cady, N. C. A novel microfluidic device for the in situ optical and mechanical analysis of bacterial biofilms. *J. Microbiol. Methods* **2012**, *91* (1), 198−204.

(59) Powell, L. C.; Sowedan, A.; Khan, S.; Wright, C. J.; Hawkins, K.; Onsøyen, E.; Myrvold, R.; Hill, K. E.; Thomas, D. W. The effect of alginate oligosaccharides on the mechanical properties of Gram-negative biofilms. *Biofouling* **2013**, *29* (4), 413−421.

(60) Vignaga, E.; Haynes, H.; Sloan, W. T. Quantifying the tensile strength of microbial mats grown over noncohesive sediments. *Biotechnol. Bioeng.* **2012**, *109* (5), 1155−1164.

(61) Zeng, G.; Vad, B. S.; Dueholm, M. S.; Christiansen, G.; Nilsson, M.; Tolker-Nielsen, T.; Nielsen, P. H.; Meyer, R. L.; Otzen, D. E. Functional bacterial amyloid increases *Pseudomonas* biofilm hydro-phobicity and stiffness. *Front. Microbiol.* **2015**, *6*.10.3389/fmicb.2015.01099

(62) Derlon, N.; Massé, A.; Escudié, R.; Bernet, N.; Paul, E. Stratification in the cohesion of biofilms grown under various environmental conditions. *Water Res.* **2008**, *42* (8), 2102−2110.

(63) Towler, B. W.; Rupp, C. J.; Cunningham, A. B.; Stoodley, P. Viscoelastic properties of a mixed culture biofilm from rheometer creep analysis. *Biofouling* **2003**, *19* (5), 279−285.

(64) Körstgens, V.; Flemming, H.-C.; Wingender, J.; Borchard, W. Uniaxial compression measurement device for investigation of the mechanical stability of biofilms. *J. Microbiol. Methods* **2001**, *46* (1), 9−17.

(65) Ohashi, A.; Koyama, T.; Syutsubo, K.; Harada, H. A novel method for evaluation of biofilm tensile strength resisting erosion. *Water Sci. Technol.* **1999**, *39* (7), 261−268.